Analysis of the Anomalous Brillet and Hall Experimental Result

Robert D. Klauber
1100 University Manor Dr., 38B, Fairfield, Iowa 52556
klauber@.iowatelecom.net, permanent: rklauber@.netscape.net

Published: *Found. Phys. Lett.* June 2004

Abstract

The persistent, second order, anomalous signal found in the Brillet and Hall experiment is derived by applying 4D differential geometry in the rotating earth frame. By incorporating the off diagonal time-space components of the rotating frame metric directly into the analysis, rather than arbitrarily transforming them away, one finds a signal dependence on the surface speed of the earth due to rotation about its axis. This leads to a Brillet-Hall signal prediction in remarkably close agreement with experiment. No signal is predicted from the speed of the earth in solar or galactic orbit, as the associated metric for gravitational orbit has no off diagonal component. To corroborate this result, a repetition by other experimentalists of the Brillet-Hall experiment, in which the test apparatus turns with respect to the earth surface, is urged.

Key Words: Brillet-Hall, relativistic rotation, anisotropic light speed, non-time-orthogonal

1 INTRODUCTION

1.1 Background

In 1978, Brillet and Hall[1] used a Fabry-Perot[2] interferometer that rotated with respect to the lab to measure the isotropy of space (i.e., of the speed of light). As the apparatus turned, anisotropic speed of light would cause otherwise coherent light waves to change phase and partially interfere, thereby reducing the transmitted wave intensity. A servo adjusted the frequency (and therefore the wavelength and phase) to maximize the transmitted wave intensity. Thus, the change in frequency was a direct measure of the degree of anisotropy.

Brillet-Hall found a "null" effect at the $\Delta f/f = 3\text{X}10^{-15}$ level, where f is the frequency of the electromagnetic wave employed and Δf is the amplitude of the change in f as the apparatus is rotated. However, to obtain this result they subtracted out an anomalous non-null signal of approximate amplitude $2\text{X}10^{-13}$ at twice the apparatus rotation rate. This signal had effectively constant phase in the laboratory (earth) frame, and though "persistent", was deemed "spurious" without further comment.

In 1981, Aspden[3] noted that this anomalous signal corresponded closely to what pre-relativity physicists would have expected solely from the earth surface velocity. According to

logic employed by Michelson and Morley[4], $\Delta f/f$ is related to $^1\!/_2 v^2/c^2$, where v is the speed of the test apparatus relative to the frame in which light speed is isotropic. Aspden suggested that perhaps in some little understood way, the earth surface speed might be somehow different in nature than the solar and galactic orbit speeds. His analysis implied that, if light speed were anisotropic, $\Delta f/f$ would have an amplitude of $(.262)(^1\!/_2 v^2/c^2)$. Setting this result equal to the measured signal of $\sim 2\text{X}10^{-13}$, one finds a v value of approximately 362 m/sec. The earth surface velocity at the test site due to rotation about the earth's axis is 355 m/sec.

The present author believes Aspden's analysis to be flawed[1][5]. Nevertheless, the detected signal is within a factor of two of what Michelson-Morley would have attributed to the earth surface velocity. (It turns out, as we will see, that $^1\!/_2 v^2/c^2$ would be peak-to-peak in the Brillet-Hall test, and half of this would be the amplitude.) In the present article, this signal is evaluated using general relativity/differential geometry in which off diagonal time-space components occur in the rotating (earth) frame metric. For such a metric, time is not orthogonal to space, and this is referred to as non-time-orthogonality. As shown below, non-time-orthogonal (NTO) analysis[6],[7] implies an anisotropy in the speed of light in rotating frames, which when applied to the earth, leads to a prediction of the observed $\sim 2\text{X}10^{-13}$ signal.

In this context, we note that as a result of studies on global positioning system (GPS) electromagnetic signal data, recognized world leading GPS expert Neil Ashby recently noted in *Physics Today*,

" .. the principle of the constancy of c cannot be applied in a rotating reference frame .." [8].

He has also stated,

"Now consider a process in which observers in the rotating frame attempt to use Einstein synchronization [constancy of the speed of light] *..... Simple minded use of Einstein synchronization in the rotating frame ... thus leads to a significant error".*[9]

It is emphasized preemptively that NTO analysis does not contravene the geometric foundation of relativity theory. In fact, it is a direct consequence of straightforward application of differential geometry to cases where time is not orthogonal to space. These include rotating frames and spacetime around a star possessing angular momentum (in which off diagonal spacetime metric components also exist.) NTO methodology leaves unchanged all analyses of systems in which time is orthogonal to space. Such systems comprise free fall frames in gravitational orbits and the vast majority of all other relativistic systems. Hence, the null signals obtained in many tests for effects of the solar or galactic orbit speeds are not in conflict with NTO analysis.

Further, NTO analysis is in complete agreement with all known experiments[10],[11],[12],[13]. Of these experiments, only the Brillet-Hall test has been capable of monitoring any effect due to non-time-orthogonality of the rotating earth fixed reference frame[2].

1.2 Analysis Approach

The steps in analysis presented herein are as follows.

[1] Aspden considered the change in angle of the output signal due to "motion of the mirror relative to the light reference frame" to be responsible for the non-null signal variation observed. However, the output signal in the Brillet-Hall experiment was monitored only for frequency change, and for an observer and apparatus fixed in the same frame, this does not vary with frame orientation, even in a Galilean analysis. (Wave speed and wavelength would change, but not frequency.) See Section 4.2 herein, ref. [3], and ref. [5].

[2] Arguments can, however, be made that the Sagnac effect (see ref. [13]) results from such non-time-orthogonality.

1. Introductory overview of NTO analysis (Section 2.)

2. Determination of physical light speed (i.e., measured with physical instruments) in the circumferential and radial directions of a rotating frame via NTO analysis. (Section 3.1), and from them, the difference in time delay for the two directions (Sections 3.2, 3.3, and 3.4.)

3. A review of the Brillet and Hall apparatus, analysis of the result predicted by the NTO approach due to differences in time delay of light signals in the radial and circumferential direction, and a comparison with the actual results. (Section 4.) The signal predicted is seen to be of the same order of magnitude but off by somewhat less than a factor of two.

4. An analysis of effects on the light signal other than time delay predicted by the NTO approach. (Section 5.) These other effects are transverse to the light propagation direction, whereas the signal time delay is a parallel direction effect. The two combined are then shown to result in a predicted signal strikingly close to that measured by Brillet and Hall.

5. An explanation for why null signals are predicted by NTO analysis for solar and galactic orbital speeds but not for the earth surface speed due to rotation about its axis. (Section 6.)

6. Summary and Conclusions (Section 7.)

2 OVERVIEW OF NTO ANALYSIS

The most widely accepted transformation[3] from the non-rotating (lab, upper case symbols) frame to a rotating (lower case) frame is

$$\begin{aligned} cT &= ct \\ R &= r \\ \Phi &= \phi + \omega t \\ Z &= z \end{aligned} \tag{1}$$

where ω is the angular velocity of the rotating frame and cylindrical spatial coordinates are used. The coordinate time t for the rotating system equals the proper time of a standard clock located in the lab, which equals the time on a standard clock at the origin (axis of rotation) of the rotating frame.

Substituting the differential form of (1) into the line element in the lab frame

$$ds^2 \;=\; -\; c^2dT^2 + \; dR^2 \;+\; R^2d\Phi^2 \;+\; dZ^2 \tag{2}$$

results in the line element for the rotating frame[4][14]

$$ds^2 \;=\; -c^2(1-\tfrac{r^2\omega^2}{c^2})dt^2 \;+\; dr^2 \;+\; r^2d\phi^2 \;+\; 2r^2\omega d\phi dt \;+\; dz^2 = \; g_{\alpha\beta}dx^\alpha dx^\beta. \tag{3}$$

[3]There is significant background behind this transformation that is discussed in greater depth in refs [6] and [7]. We shall tentatively accept this transformation as valid and find in Section 5 that it results in a correct prediction for the experiment under consideration.

[4]The first person to determine this metric for rotating frames may have been Paul Langevin [14], who used it successfully to analyze the Sagnac experiment, though he did not suggest it would lead to a non-null Michelson-Morley result for rotation. See further comments in this regard by the present author in refs [6], [7], and [13].

Note that the metric in (3) is not diagonal, since $g_{\phi t} \neq 0$, and this implies that time is not orthogonal to space (i.e., an NTO frame.) This mathematical feature becomes physically significant due to the fact that in a rotating frame it is not possible to synchronize clocks continuously without producing an NTO coordinatization. (See refs. [6] and [7].)

Time on a standard clock at any fixed 3D location in the rotating frame, found by taking $ds^2 = -c^2 d\tau$ and $dr = d\phi = dz = 0$, is

$$d\tau = d\hat{t} = \sqrt{-g_{tt}}dt = \sqrt{1 - r^2\omega^2/c^2}dt, \tag{4}$$

where the caret over dt indicates *physical* (proper) time (i.e., time measured with physical world standard clocks fixed in the rotating frame.) Obviously, time becomes imaginary for $r > c/\omega$, speed becomes faster than light, and physical clocks (or any material body) cannot exist at such locations.

3 LIGHT SPEEDS AND TRAVEL TIMES

3.1 Light Speeds in Two Directions

3.1.1 Circumferential Direction Light Speed

For light $ds^2 = 0$. Inserting this into (3), taking dr=dz=0, and using the quadratic equation formula, one obtains a light coordinate velocity (generalized coordinate spatial grid units per coordinate time unit) in the circumferential direction

$$v_{light,coord,circum} = \frac{d\phi}{dt} = -\omega \pm \frac{c}{r}, \tag{5}$$

where the sign before the last term depends on the circumferential direction of travel of the light ray. The physical velocity (the value one would measure in experiment using standard meter sticks and clocks in units of meters per second) is found from this to be[5][15]

$$v_{light,phys,circum} = \frac{\sqrt{g_{\phi\phi}}d\phi}{\sqrt{-g_{tt}}dt} = \frac{-r\omega \pm c}{\sqrt{1 - \frac{\omega^2 r^2}{c^2}}} = \frac{-v \pm c}{\sqrt{1 - \frac{v^2}{c^2}}}, \tag{6}$$

where $v = \omega r$ is the circumferential speed of a point fixed in the rotating frame as seen from the lab. Note that for rotation, the physical speed of light is not invariant or isotropic, and that this lack of invariance/isotropy depends on ω, the angular velocity. If ω=0, light speed is isotropic and invariant, the metric (3) is diagonal, and time is orthogonal to space.

3.1.2 Radial Direction Light Speed

For a radially directed ray of light, $d\phi = dz = 0$, and $ds = 0$. Solving (3) for dr/dt one obtains

$$\frac{dr}{dt} = c\sqrt{1 - r^2\omega^2/c^2}. \tag{7}$$

[5]The texts and articles listed in ref. [15] are among those that discuss physical vector and tensor components (the values one measures in experiment) and the relationship between them and coordinate components (the mathematical values that depend on the generalized coordinate system being used.) This relationship is $u^{\hat{\mu}} = \sqrt{g_{\underline{\mu\mu}}}u^{\mu}$ where the caret over the index indicates a physical vector component and underlining implies no summation.

Since $g_{rr} = 1$, the physical component (measured with standard meter sticks) for radial displacement $d\hat{r}$ equals the coordinate radial displacement dr. The physical (measured) speed of light in the radial direction is therefore

$$v_{light,phys,radial} = \frac{d\hat{r}}{d\hat{t}} = \frac{\sqrt{g_{rr}}dr}{\sqrt{-g_{tt}}dt} = \frac{dr}{\sqrt{1 - r^2\omega^2/c^2}dt} = c. \tag{8}$$

For details on NTO analysis, the reader is referred to Klauber[6],[7].

3.2 Round Trip Travel Times

3.2.1 Circumferential Round Trip Travel Time

In a given direction the outward and return round trip time over a path length l is

$$t_{RT} = \frac{l}{v_+} + \frac{l}{v_-}, \tag{9}$$

where notation should be obvious. Inserting (6) into (9), and using absolute values for speed in (6), one obtains the circumferential round trip light time

$$t_{RT,circum} = \frac{l\sqrt{1 - v^2/c^2}}{c - v} + \frac{l\sqrt{1 - v^2/c^2}}{c + v}. \tag{10}$$

This readily becomes

$$t_{RT,circum} = \frac{2lc\sqrt{1 - v^2/c^2}}{c^2 - v^2} = \frac{2l}{c\sqrt{1 - v^2/c^2}} \cong \frac{2l}{c}\left(1 + \tfrac{1}{2}\tfrac{v^2}{c^2}\right). \tag{11}$$

3.2.2 Radial Round Trip Travel Time

From (8), we know that in rotating frames for the radial direction $v_+ = v_- = c$. Using these values in (9), one finds the round trip (assuming g_{tt} is effectively constant over short distances) time, as measured on standard clocks fixed in the rotating frame, to be

$$t_{RT,radial} = \frac{2l}{c}. \tag{12}$$

This is no different from that of inertial systems in special relativity.

3.3 Round Trip Time Difference

Consider the earth as a rotating frame with either a Michelson-Morley or Brillet-Hall experiment mounted on the earth's surface. Each apparatus turns so that the perpendicular and parallel (to the earth surface speed around its axis) directions are alternately tested for the round trip light travel times.

The difference between the parallel and perpendicular directions for rotation is (11) minus (12),

$$\Delta t_{RT,NTO\ frame\ rotation} \cong \frac{2l}{c}\left(\tfrac{1}{2}\tfrac{v^2}{c^2}\right) = (t_{RT,no\ motion})\left(\tfrac{1}{2}\tfrac{v^2}{c^2}\right) = \tfrac{1}{2}\beta^2(t_{RT,no\ motion}). \tag{13}$$

3.4 Rotation vs Translation

For the NTO rotating frame analysis, the radial direction corresponds to the perpendicular direction for a translating system. Note, the travel times for this direction between Galilean translation (reviewed in Appendix B) and NTO relativistic rotation are not the same, and differ by a factor of ½ before the β^2. (Compare (12) to (46).)

Note also that the travel times between Galilean translation and NTO relativistic rotation in the parallel to velocity direction also differ by a factor of ½ before β^2 (compare (11) to (47).)

However, the difference between the parallel and perpendicular directions for both cases is (13), i.e., the same as (48). One can thus conclude that according to NTO analysis, the Michelson-Morley and Brillet-Hall experiments performed on a rotating frame (i.e., the earth) would detect signals of the same magnitude as predicted for Galilean translation.

4 BRILLET-HALL

4.1 Brillet-Hall's Fabry-Perot Interferometer

A Fabry-Perot interferometer[2] consists of two partially transmitting, partially reflecting mirrors separated by an "etalon" (of length d) and facing one another as shown in Figure 1. Light entering the left side of the Fabry-Perot interferometer in Figure 1 emerges as a series of rays on the right side, and creates a fringe pattern. For reference, a derivation of the well known constructive interference relation (shown inside the box of Figure 1 and repeated below as (14)) is provided in Appendix A.

To help make a point later, we emphasize here that a wave front entering from the left is visualized as a collection of Huygen's type wavelets. The particular ray components of such wavelets entering the left glass section at angle α produce constructive interference at an exit angle of α. Other ray components of the same wave front, entering at other angles, produce various degrees of destructive interference. In essence then, a change in angle of incidence of the centerline of a macroscopic beam of light would have no effect on the angle α at which constructive interference occurs.

The angle α of peak intensity for light exiting the Fabry-Perot interferometer is found from

$$\cos\alpha = \frac{m\lambda}{2d}, \tag{14}$$

where m, the mode number, is an integer, and different values for m correspond to different angles of local peaks in intensity.

4.2 Fabry-Perot and the Brillet-Hall Experiment

The incoming light ray depicted in the Fabry-Perot interferometer of Figure 2 has an incident angle of zero. The upper part of the figure shows the right traveling incident ray (ray #1), its left traveling reflection off of the RHS (ray #1r), and the right traveling reflection of the ray #1r (ray #2). For simplicity, additional successive rays (#2r, #3, #3r, etc.) that would result from reflection of ray #2 and subsequent reflections are not shown. Isotropy of light speed is assumed in the upper part of Figure 2, and the wavelength has been adjusted (by varying the incident light frequency) so that ray #1 and ray #2 are in phase when they strike the RHS. The portions of #1 and #2 that exit the RHS will then combine to maximize intensity of the

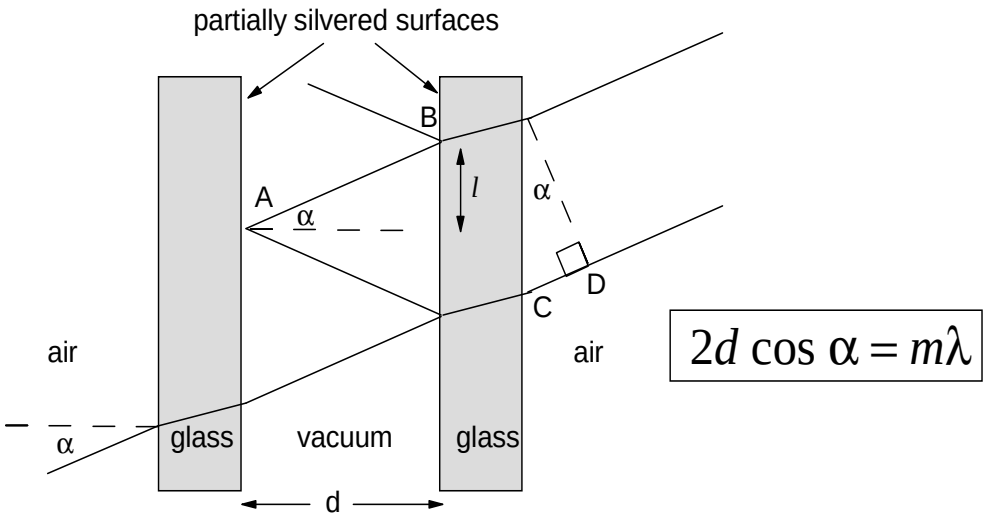

Figure 1: Fabry-Perot Interferometer

resultant beam. Higher order rays (#3, #4, etc. not shown) would then be in phase with #1 and #2 as well.

From (14), the condition for constructive interference with $\alpha = 0$ and isotropic light speed is

$$\lambda = \frac{2d}{m}. \tag{15}$$

Note that a change in either the etalon length or the wavelength will reduce the constructive interference at $\alpha = 0$ and thus, the intensity sensed.

For anisotropic light speed (lower part of Figure 2), the round trip time for a given wave maximum to reflect from the right mirror and return to the right mirror would be greater than for the isotropic case. Hence, the phase relation between waves #1 and #2 would vary as the apparatus turned, and thus so would intensity of the light entering the sensor. By judiciously changing the wavelength as the orientation changed, one could, in principle, maintain maximum constructive interference.

Brillet-Hall used this property of the Fabry-Perot interferometer to measure light speed anisotropy. They employed a He Ne generated laser that was successively reflected off two mirrors and into an Fabry-Perot interferometer, as shown in Figure 3. A sensor at fixed angle relative to the Fabry-Perot interferometer monitored the output radiation intensity, and the signal from it was fed into a servo unit. The entire apparatus shown in Figure 3 was mounted on a 95 cm by 40 cm by 12 cm granite table. The table was then turned about an axis perpendicular to the table surface at the rate of one revolution every 10 seconds. As the apparatus turned, the servo unit continually adjusted the frequency (and hence the wavelength) of the generated laser to maintain sensor intensity at a maximum. Variation in this frequency was therefore a direct measure of the anisotropy of light speed.

Thus, if light speed were anisotropic in rotating frames as NTO analysis suggests, the $\frac{1}{2}\beta^2$ of (13) would represent the fractional change in time between maxima of the first and second

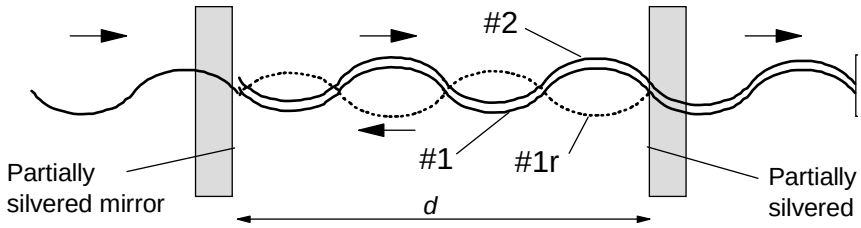

Fabry Perot Interferometer, Isotropic, Maximum Intensity

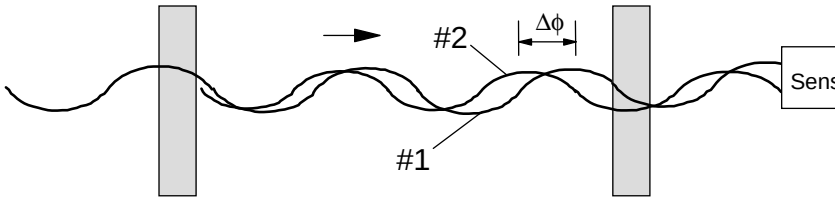

Fabry Perot Interferometer, Anisotropic Light Speed

Figure 2: Anisotropic vs Isotropic Light Speed in the Fabry-Perot Interferometer

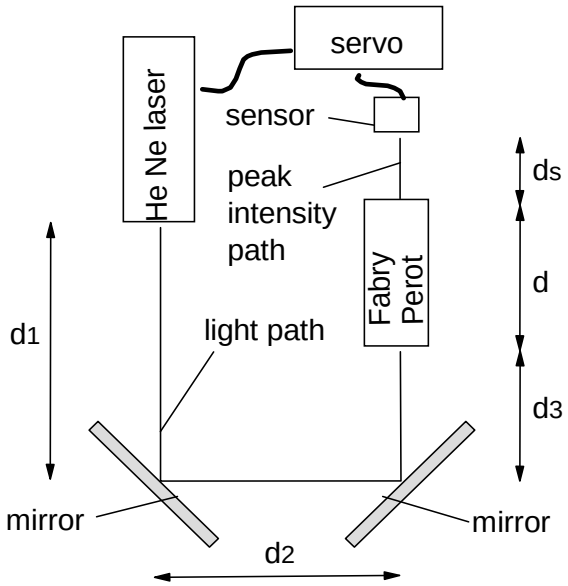

Figure 3: Schematic of the Brillet-Hall Apparatus

right traveling waves as they exit the etalon on the RHS. That is, it represents the phase lag of the second wave behind the first upon arrival at the RHS. Changing the wavelength (done by changing the frequency) can reduce this phase lag to zero and maximize the detected intensity. Hence, the amount the servo changes frequency in order to maximize intensity indicates the magnitude of $1/2\beta^2$ and therefore the magnitude of v detectable (i.e., the degree of anisotropy.)

4.3 Time Delay Due to Anisotropy in the Brillet-Hall Test

We saw in Section 3.4 that the time delay variation imparted to wave #2 in Figure 2 as a result of changing orientation of the Fabry-Perot interferometer through 90^o for both translating frames in a Galilean universe and NTO rotating frames is (13), i.e.,

$$\Delta t_{RT,moving\,frame} \cong \tfrac{1}{2}\beta^2(t_{RT,no\,motion}). \tag{16}$$

Note, however, that the Michelson-Morley apparatus has two perpendicular legs and results in (16) representing a single-sided amplitude variation in the fringing as the apparatus turns. This is a result of the lead time of one leg over the other becoming a lag time when the apparatus is turned 90^o. In the Brillet-Hall experiment, on the other hand, the round trip time difference, although numerically equal to (16), is a peak-to-peak (double-sided) amplitude. The Brillet-Hall apparatus uses a Fabry-Perot interferometer as a single arm and the time delay varies between zero for the radial direction and the same value (given by (11)) for both the positive and negative circumferential directions.

4.4 Brillet-Hall: NTO Time Delay Prediction

As Brillet-Hall noted, with a single arm interferometer, any variation due to anisotropy would have a peak-to-peak magnitude (total change) represented by the magnitude of (16). That is, since an increase in time delay must be compensated for by an increase in wavelength (i.e., a decrease in frequency),

$$\frac{\Delta t}{t} \cong \frac{\Delta\lambda}{\lambda} \cong \frac{-\Delta f}{f} \cong \frac{1}{2}\beta^2 \quad \text{(total change, Brillet-Hall)}. \tag{17}$$

This contrasts with the Michelson-Morley experiment in which there were two perpendicular arms and the peak-to-peak signal would be twice the magnitude of (17). In both experiments, this detected signal would vary with 2X the apparatus rotation rate. In the Brillet-Hall experiment the amplitude of the fractional change in frequency $\Delta f/f$ of the HeNe laser radiation source employed may thus be expected, to lowest order, to be half of the absolute value of (17), i.e

$$\frac{\Delta f}{f} \cong \frac{1}{4}\beta^2 \quad \text{(amplitude, Brillet-Hall)}. \tag{18}$$

At the location of the Brillet-Hall test, the earth surface speed is 355 m/sec. So, for $c = 3\text{X}10^8$ m/sec one finds $1/2\beta^2 = 7.00\ \text{X}10^{-13}$ (peak-to-peak). The amplitude of the fractional time delay $\Delta t/t$ $(= |\Delta f/f|\ )$ between successive exiting waves obtained as the apparatus rotates would be half of this or $3.5\ \text{X}10^{-13}$. This signal should have constant phase angle relative to the lab (earth) frame.

4.5 Billet and Hall: Test Result

The mean value of the anomalous signal Brillet-Hall measured was $\Delta f/f \cong 2 \times 10^{-13}$ at twice the table rotation rate and constant phase angle in the lab. Data varied between –42% and +52% of the mean.

The detected mean value is approximately 57% (2/3.5) of that predicted by NTO analysis of the signal time delay due to an anisotropy induced by the earth surface speed. Considering the experiment covered a range that extended to 10^{-15}, one could consider this result alone to be quite significant. However, there are additional effects on the Brillet-Hall signal predicted by NTO analysis that modify the prediction and bring it significantly closer to the measured value. These are discussed in the following section.

5 FURTHER NTO EFFECTS ON BRILLET-HALL SIGNAL

5.1 Qualitative Considerations

We emphasize that the effect of the earth surface speed on the speed of light in (6) is due to non-time-orthogonality in a rotating frame and is *not* the result of an "ether wind". However, it can aid in analysis and visualization of the effect described below if one temporarily ignores the second order contribution in (6), and thinks of the effect somewhat classically. Then the earth surface velocity $\mathbf{v}$ (magnitude v) can be effectively considered as a simple vector addition to the usual velocity (magnitude c) of a light ray.

In Figure 4 one sees the NTO effect of $\mathbf{v}$ in the Brillet-Hall experiment when it is transverse to the path of a beam of light. In the left side of the figure the portion of the incoming laser beam between the two mirrors, which we designate as "leg 2", is perpendicular to the direction of $\mathbf{v}$. The result is a deflection of the beam by an amount Δ_2 at the right hand mirror. Since the mirror is aligned at 45^o to leg 2, the same Δ_2 deflection of the beam will occur to the beam as it enters, and leaves, the Fabry-Perot interferometer. Hence, the peak intensity fringe that would otherwise strike the sensor directly is moved to the right in the figure by the amount Δ_2.

Similar effects can be seen in the right hand side of the figure for leg 1 (Δ_1 deflection) and leg 3 (Δ_3 deflection) when the apparatus mounting table is turned by 90^o relative to the earth surface. Note there is an additional effect of a change in angle of incidence for the ray as it traverses leg 3. However, as noted in section 4.1, this has no effect on the angle at which constructive interference occurs, and for our purposes, can therefore be ignored.

The important point to note is that we now have four separate effects on intensity detected by the sensor that are due to the earth surface speed. These are

1) Time delay (Section 4.4),
2) Δ_1 from transverse effect on leg 1,
3) Δ_2 from transverse effect on leg 2, and
4) Δ_3 from transverse effect on leg 3.

5.2 Quantification of Transverse Effects

Taking the orientation for $\mathbf{v}$ relative to the test table of the left side of Figure 4 as $t = 0$, and using the dimensions for each leg shown in Figure 3, the lowest order value for Δ_2 is

$$\Delta_2 = d_2 \left(\frac{v}{c}\right) \cos \omega_T t, \tag{19}$$

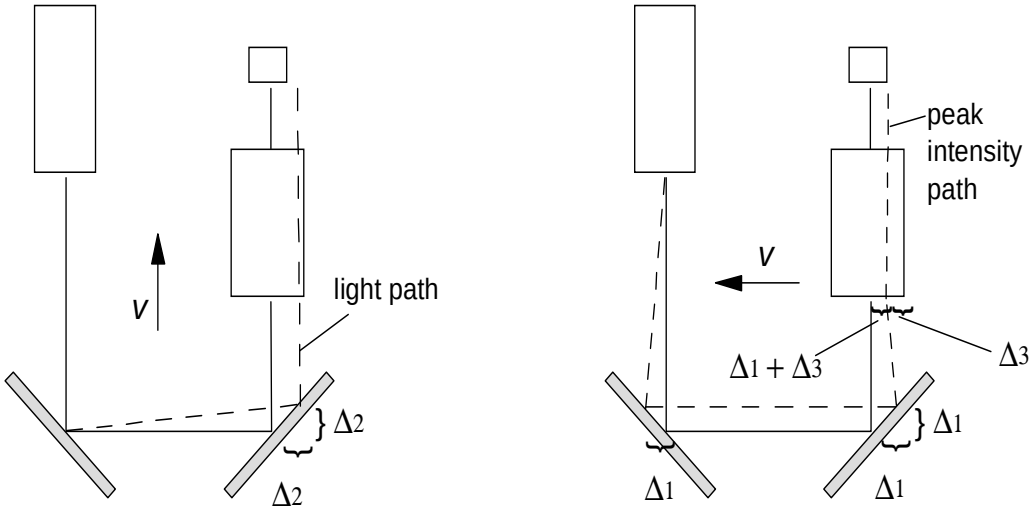

Figure 4: Transverse Effect of Earth Surface Speed on Light Path

where ω_T is the rate at which the table turns in radians/sec.

Similarly, we have for the other two legs,

$$\Delta_1 = d_1 \left(\frac{v}{c}\right) \cos\left(\omega_T t - \frac{\pi}{2}\right), \tag{20}$$

and

$$\Delta_3 = -d_3 \left(\frac{v}{c}\right) \cos\left(\omega_T t - \frac{\pi}{2}\right). \tag{21}$$

Note each of these quantities represents the respective displacement of the entire fringe pattern at the sensor location to the right of the solid line (isotropic peak intensity path) entering the sensor in Figures 3 and 4.

5.3 Cumulative Result of NTO Effects

From Figure 1, it is apparent that a decrease in wavelength increases the peak intensity angle α. Further, from Figure 2, one sees that the time delay due to anisotropy is similar in effect to a decrease in wavelength, and thus also increases the peak intensity angle. The effect of time delay on the fringe pattern is shown in the left side of Figure 5, i.e., it moves the fringes, including the peak intensity fringe, outward.

The total displacement due to transverse effects is

$$\Delta_{Transv} = \Delta_1 + \Delta_2 + \Delta_3. \tag{22}$$

The effect of positive Δ_{Transv} on the interference fringes is depicted in the right side of Figure 5, i.e., it displaces the fringes to the right. Negative Δ_{Transv} displaces the fringes to the left.

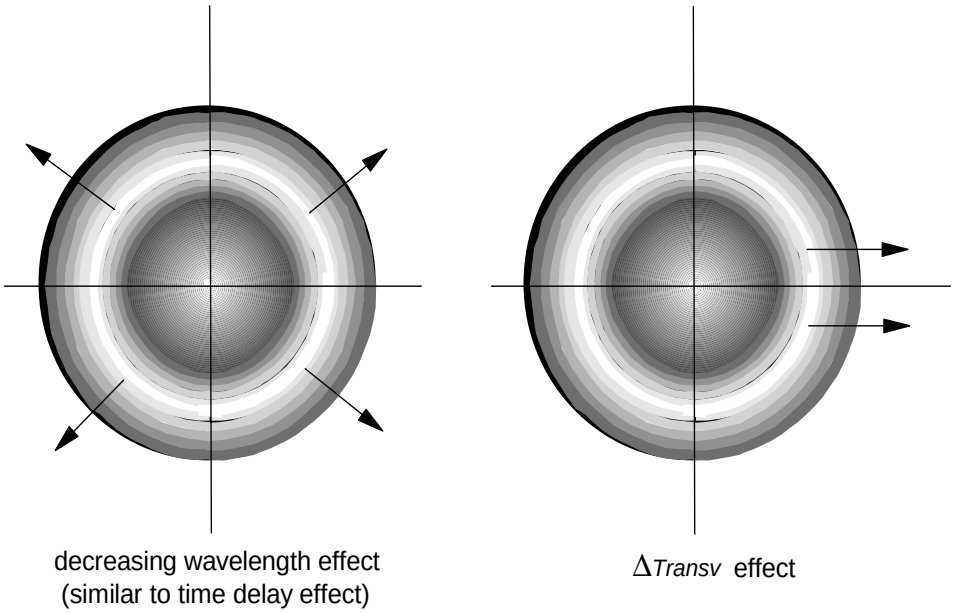

Figure 5: Effects of Interference Fringe Pattern

The peak intensity angle relation (14) can be expanded as

$$\frac{m\lambda}{2d} = \cos\alpha = \sqrt{1-\sin^2\alpha} \cong 1 - \tfrac{1}{2}\alpha^2, \tag{23}$$

since α is small. Consider, for simplicity, the ideal isotropic case in which a local peak intensity is at $\alpha = 0$ and is directed precisely at the center of the sensor. (Imagine the sensor at the origin in the left side of Figure 5, light speed is isotropic, and the peak intensity is located at the origin.) From (23) this means

$$\lambda_0 = \frac{2d}{m}, \tag{24}$$

where λ_0 is the wavelength in the isotropic case that maximizes intensity at the center of the Fabry-Perot interferometer. (For the case where α is not initially zero, see Appendix C.) Thus, from (23) and (24), we have

$$\frac{\lambda}{\lambda_0} = \frac{\lambda_0 + \Delta\lambda}{\lambda_0} \cong 1 - \tfrac{1}{2}\alpha^2 \qquad \rightarrow \qquad \tfrac{\Delta\lambda}{\lambda_0} \cong -\tfrac{1}{2}\alpha^2. \tag{25}$$

Note that $\Delta\lambda$ is always negative, and this makes sense physically. A decrease in λ means an increase in $|\alpha|$.

Consider (25) with regard to the time delay only case of Figure 2, i.e., we introduce anisotropy into our heretofore isotropic picture, but ignore transverse effects. When the Fabry-Perot interferometer is aligned in the direction of $\mathbf{v}$, the effect is similar to that of decreased λ. From our analysis of Section 4.4 and (25), we expect the relative change in wavelength to vary with an amplitude of $\beta^2/4$ between zero and a negative value of $\beta^2/2$ at twice the rate of test table rotation. From (17) and (25) then, the time delay effect on wavelength is

$$\frac{\Delta t}{t} \cong \frac{\Delta\lambda}{\lambda_0} \cong -\tfrac{1}{4}\left(\tfrac{v}{c}\right)^2 \left(\cos\left(2\omega_T t\right) + 1\right) \cong -\tfrac{1}{2}(\alpha_{TimeDelay})^2. \tag{26}$$

Trigonometry then gives us

$$(\alpha_{TimeDelay})^2 \cong \tfrac{1}{2}\left(\tfrac{v}{c}\right)^2 (\cos(2\omega_T t) + 1) = \left(\tfrac{v}{c}\right)^2 \cos^2(\omega_T t)\,, \tag{27}$$

and the variation in $\alpha_{TimeDelay}$ is

$$\alpha_{TimeDelay} \cong \pm\frac{v}{c}\cos(\omega_T t)\,. \tag{28}$$

The displacement variation at the sensor location due to time delay alone, where d_s is the distance from the exit end of the Fabry-Perot etalon to the sensor (see Figure 3), is thus

$$\Delta_{TimeDelay} \cong (d + d_s)\alpha_{TimeDelay} \cong -(d + d_s)\frac{v}{c}\cos(\omega_T t)\,. \tag{29}$$

From Figures 2, 4 and 5, we can convince ourselves that $\Delta_{TimeDelay}$ at the sensor location due to time delay is 180^o out of phase with Δ_2. Hence, from (19), we see that the proper sign in (28) and (29) is the negative one.

The total displacement then is

$$\Delta_{Tot} = \Delta_{TimeDelay} + \Delta_{transv} = \Delta_{TimeDelay} + \Delta_1 + \Delta_2 + \Delta_3 \tag{30}$$

or

$$\Delta_{Tot} = -\frac{v}{c}\left(-(d + d_s)\cos(\omega_T t) + d_1\cos\left(\omega_T t - \frac{\pi}{2}\right) + d_2\cos(\omega_T t) - d_3\cos\left(\omega_T t - \frac{\pi}{2}\right)\right). \tag{31}$$

This displacement must be corrected for by the servo to maximize intensity. That is, the servo must change the frequency, and hence the wavelength, to bring Δ_{Tot} back to zero. In other words, the induced change in wavelength must be such that if acting alone (in an isotropic world) it would produce an angle α_{Tot} that would move the peak intensity fringe by $-\Delta_{Tot}$. This angle is then

$$\alpha_{Tot} \cong \frac{-\Delta_{Tot}}{d + d_s} \cong \frac{v}{c}\left(\left(\frac{d_2 - (d + d_s)}{(d + d_s)}\right)\cos(\omega_T t) + \frac{d_1 - d_3}{(d + d_s)}\cos\left(\omega_T t - \frac{\pi}{2}\right)\right). \tag{32}$$

This can be represented as

$$\alpha_{Tot} = \frac{v}{c}A\cos(\omega_T t - \phi) \tag{33}$$

where

$$A = \frac{\sqrt{(d_2 - d - d_s)^2 + (d_1 - d_3)^2}}{d + d_s} \tag{34}$$

and ϕ is readily determinable. From (25), and a standard trigonometric relation, we have

$$\frac{\Delta f}{f_0} \cong -\frac{\Delta\lambda}{\lambda} = \tfrac{1}{2}(\alpha_{Tot})^2 = \tfrac{1}{2}\left(\tfrac{v}{c}\right)^2 A^2\cos^2(\omega_T t - \phi) = \tfrac{1}{4}\left(\tfrac{v}{c}\right)^2 A^2(1 + \cos(2\omega_T t - 2\phi))\,. \tag{35}$$

Thus, the fractional change in frequency induced by the servo varies at twice the table rotation rate at amplitude

$$\left.\frac{\Delta f}{f_0}\right|_{amplitude} = \tfrac{1}{4}\left(\tfrac{v}{c}\right)^2 A^2. \tag{36}$$

5.4 Comparison of NTO Theory with Brillet-Hall Experiment

Brillet-Hall noted that the Fabry-Perot interferometer they used had $d = 30.5$ cm, but it is unfortunate that the dimensions d_1, d_2, d_3, and d_s were not specified. However, from the schematic of their Figure 1, and knowing the dimensions of the table illustrated therein, one can make reasonable estimates for these values. For example, they appear to have values in centimeters which may be reasonably close to (d_2 appears to be between 20 and 25 cm)

$$d_s = 10 \qquad d_1 - d_3 = 25 \qquad d_2 = 22.5.$$

Then $A^2 = .58$ and

$$\left.\frac{\Delta f}{f_0}\right|_{amplitude} = .138\left(\frac{v}{c}\right)^2 = 2.03 \times 10^{-13}. \tag{37}$$

As noted in Section 4.5, the Brillet-Hall anomalous signal mean was approximately this value, and like the NTO prediction, had both constant phase (value not noted in the article) relative to the lab and variation at twice the table rotation rate.

6 GRAVITATIONAL ORBITS VS TRUE ROTATION

Why should we get a null signal for the solar and galactic orbital velocities, but a non-null signal for the earth surface speed from its own rotation? The answer is that bodies in gravitational orbits follow geodesics, i.e., they are in "free fall". That is, they are in locally inertial (time orthogonal) frames and therefore obey Lorentzian mechanics. An object in such a frame feels no force, provided it does not rotate about its own axis. There is no experimental means by which one could measure (without looking outside at the stars) one's rate of revolution (and hence one's speed in orbit).

On the other hand, objects (like the Brillet-Hall or Michelson-Morley apparatuses) fixed in "true" rotational frames are held in place by non-gravitational forces and do not travel geodesic paths. Via experiment, one can actually determine one's speed in such frames in the circumferential direction (without looking outside) in an absolute (or Machian) sense.

For example, in true rotation one can measure the motion of a Foucault pendulum's arc over time and determine the rate of rotation ω. One can also use a mass-spring system to determine the distance r to the center of rotation, and thereby calculate the circumferential speed $v = \omega r$ in an absolute sense. In gravitational orbit this can not be done. If the planet does not rotate about its own axis, there is no movement of a pendulum's arc, even thought the planet travels around its orbit. No centrifugal acceleration is felt, so one can not use a spring-mass system to determine where the center of revolution is. Hence, speed in gravitational orbit is indeterminate via experiment.

Thus, the earth surface speed is that of a true rotational system; orbital speed is not. This has at least two immediate ramifications. First, if for true rotation one can measure circumferential speed via one experiment (pendulum, spring, mass), then why not by another (Michelson-Morley or Brillet-Hall)? Second, the non-time-orthogonal factor (see off diagonal term in (3)) is a direct function of ω and r. Measuring those, we effectively measure the degree of non-time-orthogonality, and hence the degree of anisotropy.

Hence, the usual form of relativity should hold for gravitational orbits and we should expect null Michelson-Morley and Brillet-Hall results for orbital speeds, which is just what we measure.

But the NTO form of relativity theory should be applied for the earth surface speed due to rotation about the earth's axis. This issue is treated in detail in Klauber[11].

Note that the anisotropy in light speed is predicted to exist on the earth provided the earth is rotating, though it would be undetectable in practice unless the experimental apparatus turned with respect to the earth's surface, thereby enabling speed comparisons in different directions (e.g., E-W then N-S) within the rotating earth frame itself. Although other tests[16] have been performed with accuracy comparable to, or better than, that of Brillet-Hall, none of these turned the test apparatus relative to the earth surface.

7 SUMMARY AND CONCLUSIONS

Non-time-orthogonal analysis of relativistically rotating frames predicts a signal that is in accord with the anomalous non-null signal on the order of 10^{-13} found in the Brillet-Hall experiment. Contributions to the signal come from time delay and three separate transverse effects on wave propagation. Both the predicted signal and the measured signal have fixed phase in the lab frame and vary with twice the test apparatus rotation rate. Signal magnitude and phase depend on particular dimensions between components of the test apparatus, which are unknown, though estimable. Reasonable estimates for these dimensions result in a prediction that is well within the range of data found via experiment.

NTO analysis predicts a signal that is dependent on the surface velocity of the earth due to rotation about its axis, but none due to the velocity of the earth in gravitational orbit. This is in agreement with all relevant experiments. This result is due to off diagonal time-space terms that arise in the metric for true rotating frames (where angular velocity and centrifugal acceleration can be measured). No such off diagonal terms exist in the metric for bodies in the free fall frames of gravitational orbit.

This result contrasts with the null prediction of the usual relativistic analysis approach, utilizing local co-moving Lorentz frames. The Brillet-Hall measurement, GPS data, and the analysis herein raise significant questions relating to relativity theory and the nature of the spacetime continuum. (Can time truly be non-orthogonal to space, and if so, what ramifications are there for physical measurements?) The author hopes that someone will soon repeat the Brillet-Hall experiment (with apparatus rotating with respect to the earth surface) and provide definitive answers to these questions.

APPENDIX A: THE FABRY-PEROT INTERFEROMETER

For reference, this appendix provides a derivation of the well known Fabry-Perot constructive interference condition for thin films[6].

Figure 1 depicts the Fabry-Perot interferometer with two partially transmitting glass (silica) mirror sections mounted a distance d (the "etalon" length) apart. A light ray enters from the left at angle α to the horizontal, is refracted through the first glass section, and then is partially reflected at the surface of the second glass section. The reflected ray is reflected once again at A, then partially refracted at B, and upon exiting the right side of the second glass section interferes with the original refracted ray. Two phase changes of 180^o occur (at the first reflection

[6]This article does not delve into certain intricacies of geometrical optics in rotating frames, particularly with regard to reflection and half-reflection, and in this sense, derivations herein are approximate.

and the second reflection, point B) so the net phase change due to reflection upon exiting the right hand glass section is zero. The reflected portion of the ray at B leads to a third ray, as well as subsequent rays, exiting the RHS. Each successive such ray is diminished in intensity from the prior one, and the interference behavior of all of these rays together parallels that of the first two shown in Figure 1.

Note that for constructive interference, we must have

$$2AB - CD = m\lambda, \tag{38}$$

where m is an integer. The following trigonometry is straightforward.

$$AB = \frac{d}{\cos\alpha} \tag{39}$$

$$l = d\tan\alpha \tag{40}$$

$$CD = 2l\sin\alpha = 2d\tan\alpha\sin\alpha \tag{41}$$

Using the above values for AB and CD in (38), one finds

$$\frac{2d}{\cos\alpha} - 2d\tan\alpha\sin\alpha = m\lambda. \tag{42}$$

Multiplication by cosα yields

$$1 - \sin^2\alpha = \cos\alpha\frac{m\lambda}{2d}, \tag{43}$$

or

$$\frac{m\lambda}{2d} = \cos\alpha. \tag{44}$$

APPENDIX B: GALILEAN ROUND TRIP TIMES IN TRANSLATING FRAMES

The general relation for determining measured round trip travel times for different speeds in each direction is

$$t_{RT} = \frac{l}{v_+} + \frac{l}{v_-} \tag{45}$$

where l is the distance traveled in one direction measured by standard meter sticks, v_+ is the physical (measured) speed in the outward direction and v_- is the physical return speed.

Using (45), the pre-relativistic ether approach to light travel times in directions parallel and perpendicular to velocity of translation through the ether[4] yielded, to second order,

$$t_{RT,perpend} \cong \frac{2l}{c}\left(1 + \tfrac{1}{2}\tfrac{v^2}{c^2}\right) \tag{46}$$

and

$$t_{RT,parallel} \cong \frac{2l}{c}\left(1 + \frac{v^2}{c^2}\right). \tag{47}$$

The difference between these is

$$\Delta t \underset{moving\,frame}{}_{RT,\,Galilean} \cong \frac{2l}{c}\left(\tfrac{1}{2}\tfrac{v^2}{c^2}\right) = (t_{RT,no\ motion})\left(\tfrac{1}{2}\tfrac{v^2}{c^2}\right) = \tfrac{1}{2}\beta^2(t_{RT,no\ motion}) \tag{48}$$

The fractional difference in round trip light travel time between the two paths equals $^1/_2\beta^2$.

This value is reflected directly in the predicted (for classical ether) change in interference fringing in the Michelson-Morley experiment and in the change in frequency of the Fabry-Perot interferometer in the Brillet-Hall experiment. This, of course, presumes that motion in each case can be modeled as translational and Galilean.

It is significant that the Michelson-Morley experiment was not sensitive enough to detect any effect from the earth surface speed, though the Brillet-Hall experiment was.

APPENDIX C: CASE OF INITIAL PEAK INTENSITY AT $\alpha \neq 0$

Consider the case where the sensor is not located at the precise centerline of the Fabry-Perot interferometer, such that the local peak in intensity striking the sensor is not at $\alpha = 0$. That is, $\alpha_0 \neq 0$, though still small. Then

$$\frac{m\lambda_0}{2d} = \cos\alpha_0 \cong 1 - \tfrac{1}{2}\alpha_0^2 \tag{49}$$

yields the wavelength λ_o for initial peak intensity at the sensor. As the apparatus turns, due to anisotropy, the servo changes the wavelength to maintain constant α_o. The extremum value for this wavelength is λ_1, and this corresponds to what the peak intensity angle α_1 would be for such a wavelength if the apparatus had not turned. Thus,

$$\frac{m\lambda_1}{2d} = \cos\alpha_1 \cong 1 - \tfrac{1}{2}\alpha_1^2. \tag{50}$$

From (49) and (50),

$$\frac{\Delta\lambda}{\lambda_0} = \frac{\lambda_1 - \lambda_0}{\lambda_0} = \frac{\lambda_1}{\lambda_0} - 1 = \frac{\cos\alpha_1}{\cos\alpha_0} - 1 \cong \frac{1 - \frac{1}{2}\alpha_1^2}{1 - \frac{1}{2}\alpha_0^2} - 1 \cong -\tfrac{1}{2}\left(\alpha_1^2 - \alpha_0^2\right). \tag{51}$$

For

$$\alpha_1 = \alpha_0 + \Delta\alpha, \tag{52}$$

(51) becomes

$$\frac{\Delta\lambda}{\lambda_0} \cong -\tfrac{1}{2}\left((\Delta\alpha)^2 + 2(\Delta\alpha)\alpha_0\right). \tag{53}$$

The first term on the right side will cause a second order variation in $\Delta\lambda$ at twice the table rotation rate. (See (26) to (28).) The last term should cause a variation at the table rotation rate with a magnitude dependent on the initial condition α_o.

In this context, it may be significant that Brillet-Hall detected another non-null signal of magnitude $\sim$1.2X10^{-12} at the table rotation rate. They attributed this signal to gravitational stretching of their apparatus, but in light of (53), one might wonder if the cause lies elsewhere. A repetition of their test would tell us a lot.

References

[1] A. Brillet and J. L. Hall, "Improved laser test of the isotropy of space," *Phys. Rev. Lett.* **42**(9), 549-552 (1979).

[2] Useful descriptions of the Fabry-Perot interferometer can be found at http://hyperphysics.phy-astr.gsu.edu/hbase/phyopt/fabry.html and www.burleigh.com/life_science/Pages/fabryTheory.htm.

[3] H. Aspden, "Laser interferometry experiments on light speed anisotropy," *Phys. Lett.* **85A**(8,9), 411-414 (1981).

[4] See, for example, M. Born, *Einstein's Theory of Relativity* (Dover, NY, 1965), pp. 214-218.

[5] R. D. Klauber, "Frequency and Wavelength of Light in Relativistically Rotating Frames", gr-qc/0108036

[6] R. D. Klauber, "New perspectives on the relatively rotating disk and non-time-orthogonal reference frames", *Found. Phys. Lett.* **11**(5), 405-443 (1998). qr-qc/0103076.

[7] R. D. Klauber, "Toward a Consistent Theory of Relativistic Rotation", in *Relativity in Rotating Frames*, Ed. A. van der Merwe (Kluwer Academic, Dordrecht, The Netherlands, in press) http://digilander/libero.it/solciclos/

[8] N. Ashby, "Relativity and the Global Positioning System", *Phys. Today* May 2002, 41-47. See p. 44.

[9] N. Ashby, "Relativistic Effects in the Global Positioning System", *15^{th} Intl. Conf. Gen. Rel. and Gravitation,* Pune, India (Dec 15-21, 1997). Available at www.colorado.edu/engineering/GPS/Papers/RelativityinGPS.ps. See pp. 5-7.

[10] R. D. Klauber, "Non-time-orthogonality and tests of special relativity", gr-qc/0006023

[11] R. D. Klauber, "Non-time-orthogonality, gravitational orbits and Thomas precession**",** gr-qc/0007018.

[12] R. D. Klauber, "Generalized tensor analysis method and the Wilson and Wilson experiment", gr-qc/0107035.

[13] R. D. Klauber, "Derivation of the General Case Sagnac Experimental Result Using NTO Analysis", *Found. Phys. Lett.* **16**(5), 441-457 (Oct 2003). gr-qc/0206033.

[14] P. Langevin, "Théorie de l'experience de Sagnac", *Academie des sciences comptes rendus des seances* **173**, 831-834 (7 Nov 1921); "Relativité – Sur l'experience de Sagnac", **205**, 304-306 (2 Aug 1937.)

[15] R. D. Klauber, "Physical components, coordinate components, and the speed of light", gr-qc/0105071. D. Savickas, "Relations between Newtonian Mechanics, general relativity, and quantum mechanics", *Am. J. Phys.* **70**(8), 798-806. ref. [12]. ref. [6], sections 4.2.5, 4.3.3 and 5.1. C.W. Misner, K.S. Thorne, and J.A. Wheeler, *Gravitation* (Freeman, NY, 1973) e.g., see Eq. (31.5) on p. 821. I.S. Sokolnikoff, *Tensor Analysis* (Wiley, NY, 1951)

pp. 8, 122-127, 205. G.E. Hay, *Vector and Tensor Analysis*, (Dover, NY, 1953) pp 184-186. A. J. McConnell, *Application of Tensor Analysis* (Dover, NY, 1947) pp. 303-311. C. E. Pearson, *Handbook of Applied Mathematics* (Van Nostrand Reinhold, 1983 2^{nd} ed.), pp. 214-216. M. R. Spiegel, *Schaum's Outline of Vector Analysis* (Schaum) pg. 172. R. C. Wrede, *Introduction to Vector and Tensor Analysis* (Dover, NY, 1972), pp. 234-235.

[16] C. Braxmaier, H. Müller, O. Pradl, J. Mlynek, A. Peters, "Tests of Relativity Using a Cryogenic Optical Resonator", *Phys. Rev. Lett.* **88**(1), 010401-1-010401-4 (7 Jan 2002.) Also see www.uni-konstanz.de/quantum-optics/qmet/cores/mm-explain.htm.